

UCSF

UC San Francisco Previously Published Works

Title

A Wearable Patch to Enable Long-Term Monitoring of Environmental, Activity and Hemodynamics Variables

Permalink

<https://escholarship.org/uc/item/1kp8k99n>

Journal

IEEE Transactions on Biomedical Circuits and Systems, 10(2)

ISSN

1932-4545

Authors

Etemadi, Mozziyar
Inan, Omer T
Heller, J Alex
[et al.](#)

Publication Date

2016-04-01

DOI

10.1109/tbcas.2015.2405480

Peer reviewed



HHS Public Access

Author manuscript

IEEE Trans Biomed Circuits Syst. Author manuscript; available in PMC 2017 April 01.

Published in final edited form as:

IEEE Trans Biomed Circuits Syst. 2016 April ; 10(2): 280–288. doi:10.1109/TBCAS.2015.2405480.

A Wearable Patch to Enable Long-Term Monitoring of Environmental, Activity and Hemodynamics Variables

Mozziyar Etemadi [Student Member, IEEE],

Department of Bioengineering and Therapeutic Sciences, University of California, San Francisco, San Francisco, CA 94158 USA

Omer T. Inan [Member, IEEE],

School of Electrical and Computer Engineering, Georgia Institute of Technology, Atlanta, GA 30332 USA

J. Alex Heller [Member, IEEE],

Department of Bioengineering and Therapeutic Sciences, University of California, San Francisco, San Francisco, CA 94158 USA

Sinan Hersek,

School of Electrical and Computer Engineering, Georgia Institute of Technology, Atlanta, GA 30332 USA

Liviu Klein, and

Department of Medicine, University of California, San Francisco, San Francisco, CA 94131 USA

Shuvo Roy [Member, IEEE]

Department of Bioengineering and Therapeutic Sciences, University of California, San Francisco, San Francisco, CA 94158 USA

Mozziyar Etemadi: mozziyar.etemadi@ucsf.edu; Omer T. Inan: inan@gatech.edu

Abstract

We present a low power multi-modal patch designed for measuring activity, altitude (based on high-resolution barometric pressure), a single-lead electrocardiogram, and a tri-axial seismocardiogram (SCG). Enabled by a novel embedded systems design methodology, this patch offers a powerful means of monitoring the physiology for both patients with chronic cardiovascular diseases, and the general population interested in personal health and fitness measures. Specifically, to the best of our knowledge, this patch represents the first demonstration of combined activity, environmental context, and hemodynamics monitoring, all on the same hardware, capable of operating for longer than 48 hours at a time with continuous recording. The three-channels of SCG and one-lead ECG are all sampled at 500 Hz with high signal-to-noise ratio, the pressure sensor is sampled at 10 Hz, and all signals are stored to a microSD card with an average current consumption of less than 2 mA from a 3.7 V coin cell (LIR2450) battery. In addition to electronic characterization, proof-of-concept exercise recovery studies were performed with this patch, suggesting the ability to discriminate between hemodynamic and electrophysiology response to light, moderate, and heavy exercise.

Index Terms

Customized sensors; mHealth; rapid prototyping; seismocardiogram

I. Introduction

Seismocardiography is a non-invasive technique based on measuring the micro-vibrations of the chest wall for assessing left ventricular function [1]–[4], systolic and diastolic time intervals [5]–[7], and cardio-respiratory interactions [8]. The seismocardiogram (SCG) signal, first discovered in the 1960s by Bozhenko, *et al.* [9], represents the vibrations of the chest wall in response to the movement of tissue and blood, the displacement of the heart within the chest, and the coupling of acoustic energy from the valve closures into the ribcage and skin. Recently, several researchers have developed wearable systems for measuring SCG signals during normal activities of daily living using micromachined (MEMS) accelerometers, including a wearable vest for SCG measurement in the field and during sleep [10], [11], a flexible patch with SCG and electrocardiogram (ECG) measurement capability for use on the torso skin [12], and—though presented as a tool for measuring the ballistocardiogram (BCG) signal—similar approaches were demonstrated for measuring cardiogenic vibrations at the ear [13] and using sensors in Google Glass [14].

In contrast to the ECG, which measures cardiac electrophysiology, SCG offers a unique opportunity to assess the *mechanical* aspects of cardiovascular health unobtrusively, and warrants further exploration as a tool for potentially monitoring chronic cardiovascular diseases, such as heart failure (HF), at home. Studies have demonstrated that monitoring hemodynamics for HF patients can allow early detection of worsening symptoms prior to an exacerbation [15]; however, currently there is no viable solution for non-invasive hemodynamic sensing in the home setting for HF patients.

The SCG signal was first shown to be useful in enhancing the diagnostic capability of exercise stress testing for coronary artery disease (CAD) in 1992 [16], and then subsequently demonstrated as capable of evaluating exercise capacity for sports medicine [17]. Furthermore, the results of a large multicenter study demonstrated that combining SCG and ECG signals improved the predictive accuracy of detecting CAD compared to using ECG alone [18]. A wearable patch with SCG sensing for wearable hemodynamic monitoring may thus fill this important technological gap for home HF monitoring. Additionally, reduced weekly activity levels for HF patients have been shown to be a strong predictor of death [19]. An important advantage for SCG measurement is that the sensor used for its measurement—the accelerometer—also provides information on posture [20] and activity [21]; this information can thus be leveraged to enrich the assessment of the hemodynamics by not only analyzing hemodynamic parameters at rest, but also in response to changes in posture [11] and/or activity [22] (see Fig. 1). Such changes may portend HF exacerbations earlier than SCG signal changes observed at rest.

This paper describes the design of a miniature, low power system for SCG measurement that also adds another aspect of activity context to further expand on the physiological interpretations that can be made: high-resolution barometric pressure for altitude

computation. This pressure sensor will allow the detection of stair or hill climbing [23], providing a greater context for interpreting the hemodynamic data. **In fact, to the best of our knowledge, this design represents the lowest power consumption of any combined hemodynamic and activity recording hardware available**, with other wearable BCG and SCG systems consuming >20 mA average current at 3.0–3.6 V_{DC} (e.g., [12], [13]). This low power consumption—which would normally require an application specific integrated circuit (ASIC)—is achieved using commercially available parts by employing a novel design methodology for embedded systems interfacing to multiple digital and analog sensors for wearable health measurements. Consequently, it is customizable and reconfigurable, making it an appropriate tool for conducting iterative clinical and human subjects studies. We refer to this novel architecture as cUSM: Customized Universal Sensing Module. While in this work we used this architecture specifically for engineering a lower power SCG measurement system with enhanced ambient sensing capabilities, this architecture can also apply to multiple other sensing problems.

II. System Architecture and Specifications

Briefly, the cUSM consists of a microcontroller, digital and/or analog sensors, a microSD card for extended storage, and optional balun/antenna for wireless transmission. In the case of analog sensors, carefully chosen analog to digital converters are used to minimize analog circuit design and board layout.

A. Printed Circuit Board (PCB) and Design Rationale

A photo of the printed circuit board (PCB) that was designed and assembled is shown in Fig. 2(a). The block diagram showing the details of the circuit and sensors is shown in Fig. 3. A photo of electrodes being attached to the device and the device being worn on the chest is shown in Fig. 4. We used the ATMEGA1284P microcontroller (Atmel Corporation, San Jose, CA) for its large memory (16KB SRAM, 128KB flash), plethora of connectivity options, and ultra-low power consumption (600 nA deep sleep current w/active crystal), with the optional addition of an off-the-shelf Bluetooth serial port profile module or I2C to USB module for debugging and/or telemetry. All sensors were accessed over the SPI or I2C bus of the microcontroller. The microSD card was accessed over SPI, as the microcontroller does not provide an SD stack. This allows SD card access without any licensing requirements as demonstrated earlier [24]. Additionally, GPIO pins were used as external interrupt triggers which allowed the microcontroller to enter a deep sleep state until woken up by the sensor.

The on-board analog-to-digital converters (ADCs) were *not* used due to relatively high noise and low bit depth compared to external ADCs. In lieu of onboard ADCs, we chose sensors that either have a fully-digital interface, or an analog interface compatible with an external, delta-sigma A/D converter with adjustable gain and bandwidth built in. With this approach, the *sensor*, not the microcontroller, dictated the “tempo” of code execution.

For the ECG front-end, we used a dedicated analog-front-end (AFE) integrated circuit (IC) with on-board ADC (ADS1291, Texas Instruments, Dallas, TX), thus providing a fully-digital interface. This IC provides low-noise ECG amplification with high common-mode

rejection and low power consumption. For the accelerometer, we selected the BMA280 (Bosch Sensortec GmbH, Reutlingen, Germany) due to its digital output, tiny footprint ($2 \times 2 \times 0.95$ mm) and low noise floor ($120 \mu\text{g}/\text{Hz}$). For the pressure sensor, we used the MS5611-01BA03 (Measurement Specialties, Fremont, CA) because of its ultra-high resolution (0.065 mbar, corresponding to an altitude resolution of 10 cm), digital output, small size ($5 \times 3 \times 1$ mm) and low power consumption ($1 \mu\text{A}$ at 1.8–3.6 V). Example three-axis SCG (dorso-ventral, z , head-to-foot, y , and lateral, x) and ECG waveforms collected with this circuit are shown in Fig. 2(b).

The cUSM system spends most of its time in deep sleep mode, where the CPU clock is shut off and internal peripherals shut down. During deep sleep, while an external 32.768 kHz “watch” crystal remains active with a counter, it does not have an overflow interrupt as is common in many applications. Instead, the sensor or sensor ADC contains its own clocking circuitry that can often be adjusted over the SPI or I2C bus from the microcontroller. Once a sampling rate is set, an external hardware interrupt is used to wake the microcontroller when the sensor has available data. Upon awakening, the “ground truth” time is recorded from the 32.768 kHz crystal’s counter. This requires that the count increments (a multiple of the crystal’s vibration period) are *faster* than the selected sampling period *and* that the crystal’s counter overflow (256 times the count increment period for an 8-bit counter) occurs *slower* than the selected sampling period. Using such a scheme, a series of 8-bit integers are recorded, one per sample of the awakening sensor, and when loaded for post-processing, the integers can be unwrapped to reconstruct a time vector with a precision equal to the count increments.

The sensor data are placed in an internal cyclic memory buffer which can be quite large. If this buffer is full and microSD card is present, the microcontroller wakes the card and writes the buffer to the microSD. If this write process takes more time than the sampling period, it can be broken up without a loss of sampling rate [24]. The microcontroller then returns to sleep. This simple, cyclic-executive operating system allows for rapid code development, readily changeable update frequency, and nearly deterministic power consumption. It is depicted graphically in Fig. 2(c). **There is no USB stack or custom bootloader, just one .c file which can be tweaked to the exact specification required.**

To obviate the need for complex file system processing on the microcontroller, we created a very simple file system that is fully compatible with any FAT16-capable device such as a cellular phone or PC. Dubbed *oneFAT*, our file system is simply a FAT16 file system with one file that takes up the entirety of the free space on the microSD card. From the perspective of the PC or phone, when the microSD card is inserted, any programming language capable of reading binary files can readily access the data by opening the one file.

From the perspective of the microcontroller, any byte address after the start of the file is accessible without any knowledge of a file system other than this single offset value. This offset is a fixed constant for a given SD card size. The microcontroller can then organize this one “file” in a way convenient to the application while minimizing embedded code complexity.

For example, if multiple recordings are desired, the microcontroller can store the last-written address to the “first” (with file offset) address of the microSD card. Then, upon power-up, the microcontroller would first load this last-written address then begin writing at the address immediately after it. This scheme places the burden of recording separation on the computer reading the file, meaning **no external microcontroller file system library is required for *oneFAT***, conserving microcontroller code space and reducing the learning curve of the system.

B. System Specifications

We characterized the specifications of the system to determine: bandwidth and noise floor for each of the sensed parameters; power consumption; and battery life. The technical specifications are summarized in Table I. The specifications for the sensors are sufficient for enabling high quality recordings.

The total weight of the unit, including the battery, 3D-printed case, circuit board, and three gel electrodes is 38.2 g. The circuit board is 4.6 cm tall and 10.8 cm long; with the electrodes snapped on the thickness from the bottom of the electrodes to the top of the coin cell holder is 1.3 cm. The case adds 0.2 cm, making the total height with electrodes snapped in 1.5 cm.

Note that, because the device is attached to the skin, the temperature measurements cannot always be directly assumed to be representative of ambient temperature. Rather, they can be confounded by skin temperature. Accordingly, we recommend that the temperature measurements only be used to identify coarsely if the subject is in hot, mild, or cold climates when performing activities.

III. Methods and Evaluation

A. Signal Processing, Interpretation and Visualization

The interpretation of SCG signals is still an open research topic that is under investigation; nevertheless, certain parameters of the SCG have been demonstrated to be relevant for hemodynamic assessment. Specifically, changes in the RMS power of the SCG, as with the BCG, are correlated to changes in cardiac output, as demonstrated in previous studies [3], [25], and the SCG provides information on cardiac timing intervals such as pre-ejection period (PEP) and left ventricular ejection time (LVET) [26]. The PEP is derived from the ECG Q-wave to SCG Ao (aortic valve opening) peak, and LVET from the SCG Ao to Ac (aortic valve closure) peaks [7].

However, a major technical challenge impeding the extraction of these features from the SCG signal is motion artifact, associated with body movement or respiration. Our approach to extracting relevant information from the SCG signals involves pre-processing the SCG (and ECG) signals with linear filtering, detecting the R-wave peak timings from the ECG, and using these timings as a fiduciary for ensemble averaging the SCG. Then, from the ensemble averaged SCG, we extract features of interest such as RMS power and time intervals. For exercise recovery assessment, we segment the recovery time into 30-second windows with no overlap, each of which yields an ensemble averaged SCG waveform in the

dorso-ventral (z) and head-to-foot (y) directions (the lateral (x) direction acceleration signal-to-noise ratio was not sufficient for analysis or interpretation in this work).

An example set of recordings from a subject performing stair-climbing exercises and recovering following the exercises is shown in Fig. 6. This subject wore the wearable device on his chest at the sternum while climbing up 5 floors of stairs, then resting while standing still for three minutes, then repeating this three more times. All signals were recorded from the wearable during this experiment.

The ensemble average SCG heartbeats computed during the recovery period can then be stacked vertically, with slight offset between them, to visualize the changes in timing intervals, waveform shape, and wave amplitudes during the recovery period (see Fig. 6, bottom).

To detect the changes in altitude (gradation) during the activity, the changes in barometric pressure are measured and input to the following barometric formula:

$$z = -\frac{RT}{Mg} \ln \left(\frac{P}{P_0} \right) \quad (1)$$

where z is the change in altitude, R is the universal gas constant, T is the ambient temperature, M is the molar mass of air on Earth, P is the final pressure reading, g is the acceleration due to gravity, and P_0 is the pressure reading before the activity. The temperature that is sensed by the wearable device is confounded by the skin temperature of the user, since the device is worn on the torso skin. Accordingly, the temperature measurement mainly reflects ambient temperature, but the accuracy is limited in particular during activity. We thus recommend that the temperature measurement simply be used to derive three levels of ambient temperature at which the activity was completed: high ($T > 36^\circ\text{C}$), medium ($20^\circ\text{C} < T < 36^\circ\text{C}$), and low ($T < 20^\circ\text{C}$). These values are chosen to segment the ambient temperature range based on physiological studies that characterized skin blood flow response, determining which ambient conditions led to greater stress on the cardiovascular system [27].

B. Proof-of-Concept Recordings

We obtained approval from both the University of California, San Francisco and the Georgia Institute of Technology Institutional Review Boards (IRBs) to test the device on human subjects to perform an initial evaluation of signal quality and feasibility. The aim was to conduct preliminary studies to assess whether changes in hemodynamics could be captured by the device. Accordingly, we conducted the following as a proof-of-concept of the system: examining the hemodynamics and cardiac time intervals in response to (1) walking at a pace of 6.4 km/hr (at 15.5°C) for 1 km with no incline; (2) walking at the same pace and duration with no incline outdoors on a warm day (at 32°C); (3) walking at a similar pace (5.5 km/hr) and duration (750 m) at a slight incline (115 m elevation) outdoors in cool temperature (18.5°C). Additionally, as an unexpected result, one subject had multiple arrhythmias (premature ventricular contractions, PVCs) during the recordings; accordingly, the effects of these arrhythmias on the measurements are also presented and discussed.

While commercially available systems such as the Zephyr BioPatch (Zephyr Technology, Annapolis, MD) and the Basis B1 Watch (Basis Science, Inc., San Francisco, CA) monitor heart rate and body acceleration, they could potentially miss these subtler physiological responses that are captured by the SCG and pressure sensor. These physiological responses are well-known based on measurements in laboratory settings; thus our goal was simply to demonstrate a proof-of-concept that the measurements could also be taken with this device in the field, and that the results expected based on laboratory studies were mirrored in the results obtained with the wearable device.

IV. Results and Discussion

A. Results from Proof-of-Concept Recordings

The results from the three exercise recovery recordings from a healthy subject are shown in Fig. 6. For each of the three studies, the following is plotted (from top to bottom) during the recovery period: heart rate (HR, bpm), RMS power of the ensemble averaged (30 seconds) SCG in the dorso-ventral (top, z) and head-to-foot (bottom, y) directions, and ensemble average (30 seconds) SCG signals throughout the recovery period. The effects of the exercise on HR and hemodynamics were most pronounced in the third activity (walking uphill), and least in the first activity (walking on flat ground at a comfortable temperature). Importantly, the three different types of activities produced unique signatures in the *ambient* sensing on-board the system—the first activity showed that the subject was walking (based on the accelerometer tracings), that the altitude was not changing (based on the high resolution pressure sensor), and that ambient temperature was comfortable (based on the temperature sensor); the second showed walking, no change in altitude, and higher ambient temperature; the third showed walking, changes in altitude (precisely measured with the pressure sensor), and comfortable temperature.

Our expectation, based on laboratory studies from the existing literature, was that stroke volume and sympathetic tone would increase most for experiment (3) and least for experiment (1), and take the longest time to recover to baseline for experiment (3) and shortest time to recovery for experiment (1), and that our hardware would allow both the detection of which test was conducted and an assessment of the actual response. This was due to the fact that the hotter ambient temperature would create a lower gradient between skin temperature and ambient temperature, causing a greater demand for increased skin blood flow for thermoregulation [28], [29]; and that the incline would require higher work to complete the same walking activity. The subtle differential effects of these stressors, compared to the exercise itself, on the cardiovascular system would be most prominent in observing the mechanics of the heart's pumping and the vasculature: increased skin blood flow will lead to reduced cardiac filling, causing a greater compensatory increase in sympathetic tone in response to the same activity; additionally, increased work leads to greater heat generation in the skeletal muscles, and thus even higher skin blood flow.

The ability to measure these parameters provides the necessary context for examining and assessing the cardiovascular response to the activity appropriately. For example, if only acceleration signals were measured (and not altitude changes), then the response to the third activity may be seen as anomalous compared to the first: the subject's heart responds much

more strongly to this activity in terms of HR and hemodynamics, but this is simply due to the fact that the walk is actually uphill. The system we describe here is, to the best of our knowledge, the first that combines this level of in-depth and multi-modal assessment of activity-contextualized electrophysiology (ECG) and hemodynamics (SCG) with both sufficiently small size and long battery life to enable long-term (multi-day) measurements.

B. Premature Ventricular Contractions (PVCs)

Fig. 7 shows ensemble averaged SCG waveforms in the dorso-ventral (z) and head-to-foot (y) direction for a healthy subject, with normal beats (top), and PVCs (bottom). Note the difference in the axis scale for the two types of beats, with the PVCs resulting in significantly lower amplitude SCG beats compared to the normal. This proof-of-concept data suggests that the system described in this paper provides sufficient sensitivity in the accelerometer recordings to discriminate between normal and arrhythmic beats in both the amplitude and time-domain for SCG signals.

C. Limitations

The SCG signals measured by the patch represent inherently small (mg level) accelerations of the torso, which can be overwhelmed by motion artifacts and other interferences. For this reason, we have focused on exercise *recovery* rather than exercise itself as the medium for evaluating activity-contextualized hemodynamics. Nevertheless, if motion artifacts can be automatically detected and cancelled, then the hemodynamic response *during* exercise could be computed, which could potentially enhance the physiological assessment of the user. Another limitation is where the sensor can be placed on the body: currently, SCG signals are only well-understood when measured at the sternum or, in select studies, at the point of maximal inflection (PMI). However, these are not the most comfortable locations for the subject to wear the device, and are thus not ideal. Other related research we are currently conducting includes the investigation of ballistocardiogram (BCG) signal measurement with wearable accelerometers, at *any* position on the upper body [30]. If successful, this could greatly relax the positional constraints on the device, and allow more comfortable locations—such as the clavicle, or potentially the wrist with a smart watch—to be used with the system described here for wearable hemodynamic monitoring. Another limitation is that the human factors and usability aspects of the design have not yet been explored; this will be addressed in future work through focus groups and user surveys.

The primary limitation to the cUSM approach is the requirement of an engineering team—the cUSMs are not readily configured by a clinician. In situations where a small team is not available, a fully customizable solution such as SHIMMER can be configured by a clinician at the expense of power, sample rate, etc. as discussed in this work. As more devices are built using the cUSM platform, common denominators such as batteries, easy-to-interface sensors, etc. will yield simpler and quicker design cycles with smaller engineering teams.

This limitation aside, the cUSM architecture represents end-to-end optimization of sensor data acquisition pipeline; from the flexibility in sensor selection, to the simplicity of the code structure, to the ultra-lightweight filesystem, every attempt was made to streamline the process of obtaining subject data in a clinical environment unsupervised by an engineer.

With a growing shortage of physicians, an increase in the connectivity of devices, a greater emphasis is being placed on unobtrusive home monitoring of physiology. We believe cUSMs will catalyze future innovation in this area by rapidly assessing the clinical utility of various physiologically relevant signals, acting as a gateway to randomized controlled studies that determine tomorrow's standard of care.

V. Conclusion and Future Work

In future work, we will design mechanical packaging to encapsulate the wearable PCB, providing a water-resistant seal. We will then take measurements from HF patients in clinic, and have the patients take the device home with them after discharge for continuous assessment during normal daily activities and sleep. Particular attention will be paid to the responses of the cardiovascular system to minute exercise triggers such as going up a flight of stairs. The data will be stored on the SD card, and a rechargeable battery will be used.

This paper presents a novel combination of sensing modalities integrated on a low-power digital circuit architecture using discrete components. The design may address several technological gaps in the area of wearable technologies for health monitoring by combining electrical and mechanical measures of cardiovascular performance, with the necessary activity context based on high resolution pressure and acceleration data. We believe that such hardware can provide meaningful data regarding the condition of HF patients at home, and can be used in the future for improving the treatment of patients via closed-loop therapies and titration of care.

Acknowledgments

M. Etemadi was supported by the NIH MSTP fellowship (T32GMO7618). This work was supported by NIH/NCRR UCSF-CTSI Grant UL1 RR024131, NIH STTR Grant 1R41HL110466, FDA P50 Grant 2P50FD003793, the CIMIT 2012 Prize for Primary Healthcare Competition, and by the National Center for Advancing Translational Sciences, National Institutes of Health, through UCSF-CTSI Grant UL1 TR000004. This paper was recommended by Associate Editor S. Leonhardt.

The authors would like to thank R. Fechter, Dr. M. Harrison, Dr. D. Miniati, Dr. E. Shue, Dr. S. Schecter, Dr. T. DeMarco, and Dr. M. Janmohamed for their useful discussions and clinical guidance.

References

1. Salerno DM, Zanetti J. Seismocardiography for monitoring changes in left ventricular function during ischemia. *CHEST J.* 1991; 100:991–993.
2. Tavakolian, K. PhD dissertation. Applied Science: School of Engineering Science, Simon Fraser Univ; Burnaby, BC, Canada: 2010. Characterization and analysis of seismocardiogram for estimation of hemodynamic parameters.
3. Castiglioni, P.; Faini, A.; Parati, G.; Di Rienzo, M. Wearable seismocardiography. *Proc. 29th Annu. Int. Conf. IEEE Engineering in Medicine and Biology Society*; 2007; p. 3954-3957.
4. Inan OT, Migeotte PF, Park K-S, Etemadi M, Tavakolian K, Casanella R, et al. Ballistocardiography and seismocardiography: A review of recent advances. *IEEE J Biomed Health Inform.* to be published.
5. Crow RS, Hannan P, Jacobs D, Hedquist L, Salerno DM. Relationship between seismocardiogram and echocardiogram for the events in the cardiac cycle. *Amer J Noninvas Cardiol.* 1994; 8:39–46.
6. Di Rienzo, M.; Vaini, E.; Castiglioni, P.; Meriggi, P.; Rizzo, F. Beat-to-beat estimation of LVET and QS2 indices of cardiac mechanics from wearable seismocardiography in ambulant subjects. *Proc. 35th Annu. Int. Conf. IEEE Engineering in Medicine and Biology Soc.*; 2013; p. 7017-7020.

7. Tavakolian K, Dumont GA, Houlton G, Blaber AP. Precordial vibrations provide noninvasive detection of early-stage hemorrhage. *Shock*. 2014; 41:91–96. [PubMed: 24434413]
8. Pandia K, Inan OT, Kovacs GTA, Giovangrandi L. Extracting respiratory information from seismocardiogram signals acquired on the chest using a miniature accelerometer. *Phys Meas*. 2012; 33:1643.
9. Bozhenko BS. Seismocardiography—A new method in the study of functional conditions of the heart [Article in Russian]. *Ter Arkh*. 1961; 33:55–64. [PubMed: 13872234]
10. Di Rienzo, M.; Meriggi, P.; Rizzo, F.; Vaini, E.; Faini, A.; Merati, G., et al. A wearable system for the seismocardiogram assessment in daily life conditions. *Proc. 33rd Annu. Int. Conf. IEEE Engineering in Medicine and Biology Soc.*; 2011; p. 4263-4266.
11. Rienzo MD, Vaini E, Castiglioni P, Merati G, Meriggi P, Parati G, et al. Wearable seismocardiography: Towards a beat-by-beat assessment of cardiac mechanics in ambulant subjects. *Auton Neurosci*. 2013; 178:50–69. [PubMed: 23664242]
12. Chuo Y, Marzencki M, Hung B, Jaggernauth C, Tavakolian K, Lin P, et al. Mechanically flexible wireless multisensor platform for human physical activity and vitals monitoring. *IEEE Trans Biomed Circuits Syst*. 2010; 4:281–294. [PubMed: 23853374]
13. He, DD.; Winokur, ES.; Sodini, CG. A continuous, wearable, wireless heart monitor using head ballistocardiogram (BCG) and head electrocardiogram (ECG). *Proc. 33rd Annu. Int. Conf. IEEE Engineering in Medicine and Biology Soc.*; 2011; p. 4729-4732.
14. Hernandez, J.; Li, Y.; Rehg, JM.; Picard, RW. BioGlass: Physiological parameter estimation using a head-mounted wearable device. *Proc. MobiHealth Conf.*; Athens, Greece. 2014.;
15. Adamson PB, Magalski A, Braunschweig F, Böhm M, Reynolds D, Steinhaus D, et al. Ongoing right ventricular hemodynamics in heart failure: clinical value of measurements derived from an implantable monitoring system. *J Amer College Cardiol*. 2003; 41:565–571.
16. Salerno DM, Zanetti JM, Poliac LC, Crow RS, Hannan PJ, Wang K, et al. Exercise seismocardiography for detection of coronary artery disease. *Amer J Noninvas Cardiol*. 1992; 6:321–330.
17. Libonati JR, Ciccolo J, Glassberg J. The Tei index and exercise capacity. *J Sports Med*. 2001; 41:108–113.
18. Wilson RA, Bamrah VS, Lindsay J Jr, Schwaiger M, Morganroth J. Diagnostic accuracy of seismocardiography compared with electrocardiography for the anatomic and physiologic diagnosis of coronary artery disease during exercise testing. *Amer J Cardiol*. 1993; 71:536–545. [PubMed: 8438739]
19. Walsh JT, Charlesworth A, Andrews R, Hawkins M, Cowley AJ. Relation of daily activity levels in patients with chronic heart failure to long-term prognosis. *Amer J Cardiol*. 1997; 79:1364–1369. [PubMed: 9165159]
20. Curone D, Bertolotti GM, Cristiani A, Secco EL, Magenes G. A real-time and self-calibrating algorithm based on triaxial accelerometer signals for the detection of human posture and activity. *IEEE Trans Inf Technol Biomed*. 2010; 14:1098–1105. [PubMed: 20483689]
21. Bouarfa L, Atallah L, Kwasnicki RM, Pettitt C, Frost G, Guang-Zhong Y. Predicting free-living energy expenditure using a miniaturized ear-worn sensor: An evaluation against doubly labeled water. *IEEE Trans Biomed Eng*. 2014; 61:566–575. [PubMed: 24108707]
22. Froelicher, VF.; Myers, J. *Exercise and the Heart*. 5. Philadelphia, PA, USA: Saunders; 2006.
23. Lowe SA, ÓLaighin G. Monitoring human health behaviour in one's living environment: A technological review. *Med Eng Phys*. 2014; 36:147–168. [PubMed: 24388101]
24. Etemadi M, Heller JA, Schecter SC, Shue EH, Miniati D, Roy S. Implantable ultralow pulmonary pressure monitoring system for fetal surgery. *IEEE Trans Inf Technol Biomed*. 2012; 16:1208–1215. [PubMed: 22801521]
25. Inan OT, Etemadi M, Paloma A, Giovangrandi L, Kovacs GTA. Non-invasive cardiac output trending during exercise recovery on a bathroom-scale-based ballistocardiograph. *Phys Meas*. 2009; 30:261.
26. Zanetti, JM.; Salerno, DM. Seismocardiography: A technique for recording precordial acceleration. *Proc. 4th Annu. IEEE Symp. Computer-Based Medical Systems.*; 1991; p. 4-9.

27. Nadel ER, Cafarelli E, Roberts MF, Wenger CB. Circulatory regulation during exercise in different ambient temperatures. *J Appl Phys.* 1979; 46:430–437.
28. Rowell LB, Murray JA, Brengelmann GL, Kraning KK. Human cardiovascular adjustments to rapid changes in skin temperature during exercise. *Circulat Res.* 1969; 24:711–724. [PubMed: 5770258]
29. Adolph, E. *Physiology of Man in the Desert.* New York, NY, USA: Interscience; 1947.
30. Wiens A, Etemadi M, Roy S, Klein L, Inan OT. Towards continuous, non-invasive assessment of ventricular function and hemodynamics: Wearable ballistocardiography. *IEEE J Biomed Health Inform.* to be published.

Biographies



Moziyar Etemadi (S'07) received the B.S. and M.S. degrees in electrical engineering from Stanford University, Stanford, CA, USA, in 2008 and June 2009, respectively, and the Ph.D. degree in bioengineering from the University of California, San Francisco (UCSF), USA/ University of California, Berkeley, USA, Joint Graduate Group in Bioengineering in 2013, as part of the joint M.D./Ph.D. program.

After a short leave from the M.D./Ph.D. program, during which he was a postdoctoral scholar jointly mentored between UCSF Bioengineering and Therapeutic Sciences and UC Berkeley Electrical Engineering and Computer Sciences, he is now completing M.D. training as a third-year student at UCSF. His current research interests include translational biomedical engineering for in-home monitoring of disease and biomedical instrumentation for fetal surgery.

Dr. Etemadi was named *Forbes* magazine's "30 Under 30" in Science in January 2012. Later that year, he was awarded the Center for Integration of Medicine and Innovative Technology (CIMIT) Prize for Primary Care Innovation, and the grand prize in the Dow Sustainability Student Innovation Challenge. In 2011, he helped lead a research team in the Vodafone Americas Wireless Innovation Challenge and the mHealth Alliance Award to second prize. In 2009, while at Stanford University, he received the Frederick E. Terman Award for Scholastic Achievement in Engineering and also received the Electrical Engineering Fellowship, providing full support for his graduate studies.



Omer T. Inan (S'06–M'09) received the B.S., M.S., and Ph.D. degrees in electrical engineering from Stanford University, Stanford, CA, USA, in 2004, 2005, and 2009, respectively.

He joined ALZA Corporation (A Johnson and Johnson Company) in 2006 as an Engineering Intern in the Drug Device Research and Development Group, where he designed micropower, high efficiency circuits for iontophoretic drug delivery, and researched options for closed-loop drug delivery systems. In 2007, he joined Countryman Associates, Inc., Menlo Park, CA, USA, where he was a Chief Engineer, involved in designing and developing high-end professional audio circuits and systems. From 2009 to 2013, he was also a Visiting Scholar in the Department of Electrical Engineering, Stanford University. Since 2013, he has been an Assistant Professor of electrical and computer engineering, and a Program Faculty in the Interdisciplinary Bioengineering Graduate Program, Georgia Institute of Technology, Atlanta, GA, USA. His research interests include noninvasive physiologic monitoring for human health and performance, and applying novel sensing systems to chronic disease management and pediatric care. He has published 40 technical articles in peer-reviewed international journals and conferences, and has two issued and three pending patents.

Dr. Inan is an Associate Editor of the IEEE Journal of Biomedical and Health Informatics and the IEEE Engineering in Medicine and Biology Conference, member of the IEEE Technical Committee on Translational Engineering for Healthcare Innovation, and Technical Program Committee member or Track Chair for several other major international biomedical engineering conferences. He received the Gerald J. Lieberman Fellowship (Stanford University) in 2008–2009 for outstanding scholarship, teaching, and service. He is a three-time National Collegiate Athletic Association All-American in the discus throw and a former cocaptain of the Stanford University track and field team.



J. Alex Heller (S'12–M'13) received the B.S. degree in mechanical engineering from the University of Southern California, Los Angeles, CA, USA, and the M.S. degree in

bioengineering from the University of California, San Francisco (UCSF)/UC Berkeley Joint Graduate Group in bioengineering in 2008 and 2013, respectively.

In 2008, he joined Northrop Grumman, Marine Systems, Sunnyvale, CA, USA, as a Mechanical Engineer. Since 2010, he has worked as an Engineer and Researcher at UCSF for the Biodesign Laboratory and the Pediatric Device Consortium. His current research is focused on medical devices, specifically, on renal replacement therapy, home monitoring of chronic disease, and obstetrics related devices.



Sinan Hersek received the B.S. degree in electrical and electronics engineering from Bilkent University, Ankara, Turkey, in 2013.

He was an undergraduate Research Assistant in the National Magnetic Resonance Research Center (UMRAM) at Bilkent University. During his years in UMRAM, he worked on the development of efficient on-coil digital power amplifiers for magnetic resonance imaging devices. During his last year at Bilkent, he joined the Power Amplifier Development Department of ASELSAN (a military electronics company in Ankara, Turkey) as a part-time Engineer. Currently, he is working toward the Ph.D. degree in the School of Electrical and Computer Engineering at the Georgia Institute of Technology, Atlanta, GA, USA. His research focus is biomedical instrumentation. He is supervised by Dr. Omer T. Inan.



Liviu Klein was born in Brasov, Romania. He received the B.S. degree in mathematics and computer programming from Grigore Moisil National IT College, Brasov, Romania, the M.D. degree from the Carol Davila School of Medicine, Bucharest, Romania, and the M.S. degree in clinical investigation from Northwestern University, Evanston, IL, USA, in 1992, 1998, and 2005, respectively.

He trained in cardiovascular disease, cardiovascular epidemiology, cardiac electrophysiology, and advanced heart failure and transplantation at Northwestern University, and joined its faculty in 2009. He was the Director of the Heart Failure Device Program and established a remote heart failure device clinic, contributing to a successful

increase in device utilization and a decrease in heart failure and arrhythmia readmissions. In 2011, he was recruited to the University of California, San Francisco (UCSF), USA, to direct the Mechanical Circulatory Support and Heart Failure Device Program. His current research interests include the development of sensors and devices for remote monitoring and management of patients with cardiovascular diseases.

Dr. Klein is a member of the American Heart Association, Heart Failure Society of America, and International Society for Lung and Heart Transplant. At UCSF, he was an Assistant Professor of Medicine. He has authored work in more than 60 publications, and received several research awards and funding for research from several device companies, as well as the American Heart Association and National Institutes of Health.



Shuvo Roy (M/96) received the B.S. degree (magna cum laude with general honors for triple majors) in physics, mathematics (special honors), and computer science from Mount Union College, Alliance, OH, USA, in 1992, and the M.S. degree in electrical engineering and applied physics and the Ph.D. degree in electrical engineering and computer science from Case Western Reserve University, Cleveland, OH, USA, in 1995 and 2001, respectively.

Currently, he is a Professor in the Department of Bioengineering and Therapeutic Sciences (BTS), a joint department of the Schools of Pharmacy and Medicine at the University of California, San Francisco (UCSF), and Director of the UCSF Biomedical Microdevices Laboratory. He holds the Harry Wm. and Diana V. Hind Distinguished Professorship in Pharmaceutical Sciences II in the UCSF School of Pharmacy. He is a founding member of the UCSF Pediatric Devices Consortium, which has a mission to accelerate the development of innovative devices for children's health, and a faculty affiliate of the California Institute for Quantitative Biosciences (QB3). From 1998 to 2008, he was Co-Director of the BioMEMS Laboratory in the Department of Biomedical Engineering at the Cleveland Clinic, Cleveland, OH, USA, where he worked with basic scientists, practising clinicians, and biomedical engineers to develop MEMS solutions to high-impact medical challenges. While pursuing his Ph.D. degree, he conducted research in the areas of design, microfabrication, packaging, and performance of MEMS for harsh environments. He also investigated microstructural characteristics and mechanical properties of MEMS materials, developed the requisite microfabrication technologies, and demonstrated operation of the first surface micromachined silicon carbide transducers at high temperatures (up to 950 C). He has also developed miniaturized micro-relays for high-performance electrical switching and ice detection sensors for aerospace applications. In 2008, he joined UCSF to continue the development of biomedical devices including wireless physiological monitoring systems

and bioartificial replacement organs, and participate in the training of professional students in the School of Pharmacy as well as graduate students in the UCSF/UCB Joint Graduate Group in Bioengineering. He has contributed to more than 90 technical publications, coauthored three book chapters, been awarded 16 U.S. patents, and given more than 70 invited presentations.

Dr. Roy is an Associate Editor of *Biomedical Microdevices* and editorial board member of *Sensors and Materials*. He was the recipient of a Top 40 under 40 award by *Crains Cleveland Business* in 1999 and the Clinical Translation Award at the 2nd Annual BioMEMS and Biomedical Nanotechnology World 2001 meeting. In 2003, he was selected as a recipient of the TR100, which features the world's 100 Top Young Innovators as selected by *Technology Review*, the Massachusetts Institute of Technology's Magazine of Innovation. In 2004, he was presented with a NASA Group Achievement Award for his work on harsh environment MEMS. In 2005, he was named as a Who's Who in Biotechnology by *Crains Cleveland Business*. In 2009, he was nominated for the Biotechnology Industry Organization's Biotech Humanitarian Award, which is given in recognition of an individual who has used biotechnology to unlock its potential to improve the earth.

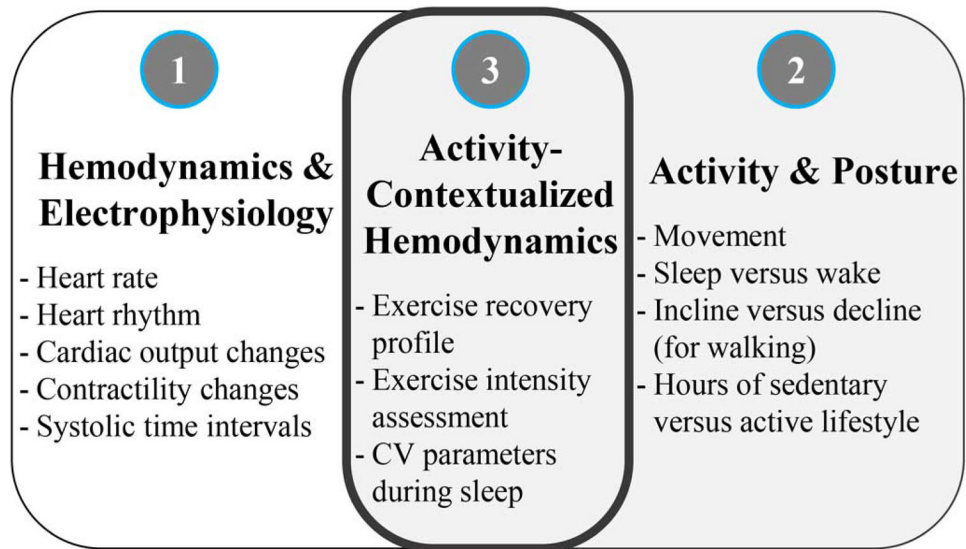


Fig. 1. Overview of key cardiovascular (1), activity/posture (2), and activity-contextualized hemodynamics (3) parameters that can be measured by the sensing suite described in this paper. These parameters can be useful for home monitoring of patients with chronic cardiovascular diseases or conditions (such as heart failure), as well as for the general population to assess personal health and fitness more accurately.

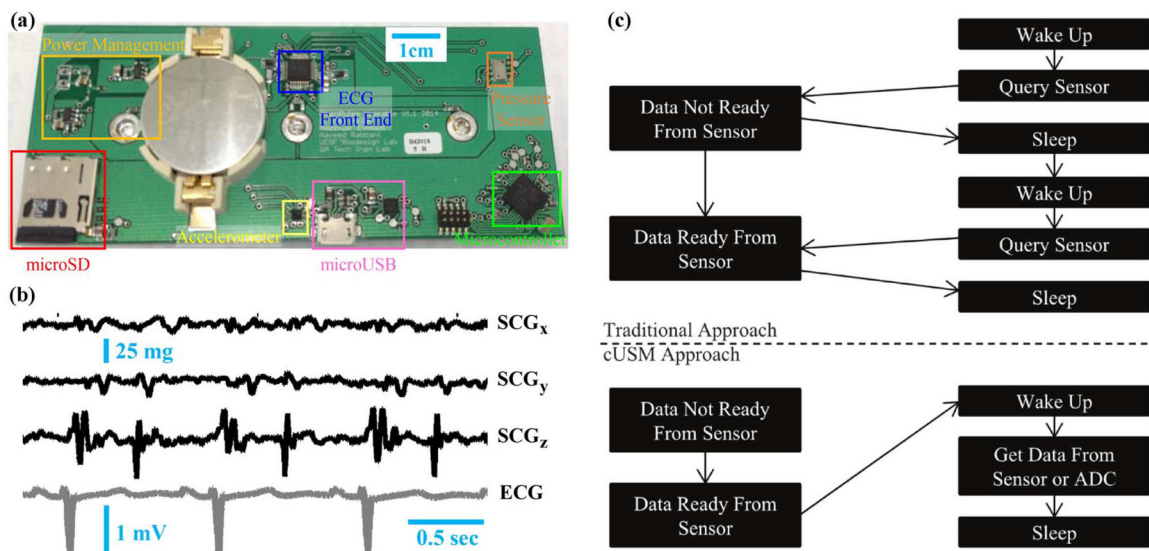


Fig. 2. (a) Photo of wearable patch hardware; this circuit includes snaps for interfacing to three Ag/AgCl gel electrodes attached to the skin. (b) Raw (unfiltered) ECG and three-axis low pass filtered ($f_c = 40$ Hz) SCG signals from one subject with the device attached to the sternum. (c) cUSM's cyclic executive operating system. In contrast to traditional approaches where timing is determined by the microcontroller, the sensor (or sensor ADC) determines the timing of the cUSM system. Writing to microSD, which is an infrequent event, is identical in both cases and is not shown.

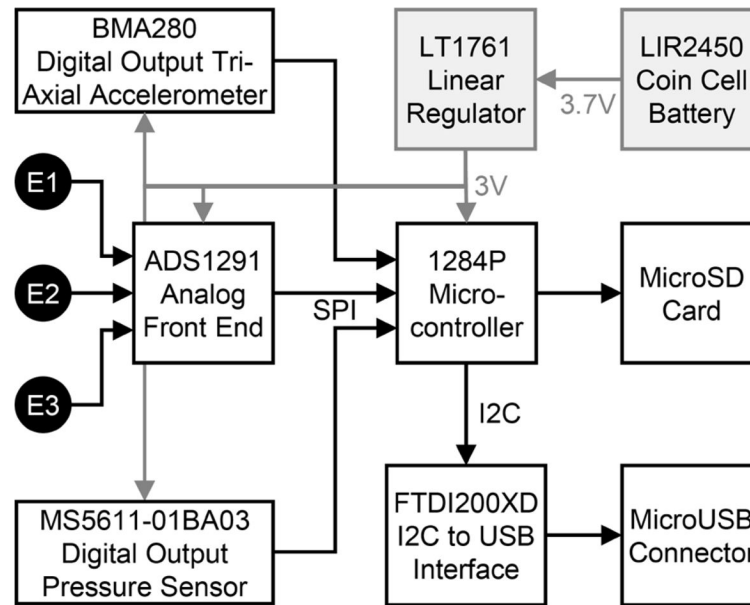


Fig. 3. Block diagram of sensors and electronic components on wearable patch. The microUSB was used for debugging purposes only. E1, E2, and E3 represent the three electrodes used for mounting the sensor on the body; SPI refers to serial peripheral interface; I2C is the inter-integrated circuit protocol; MicroSD is a micro secure digital card.

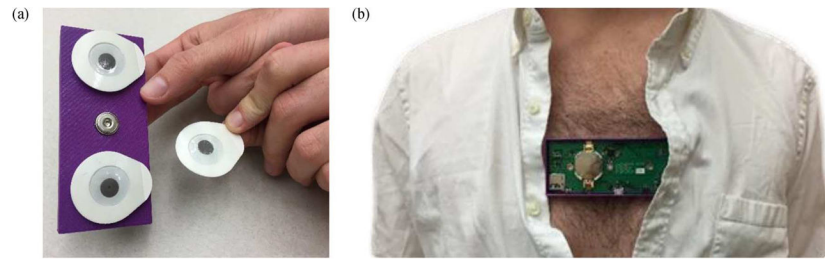


Fig. 4. (a) Placing surface ECG electrodes (Ag/AgCl) on the wearable patch snaps. (b) Photo showing device worn on the chest.

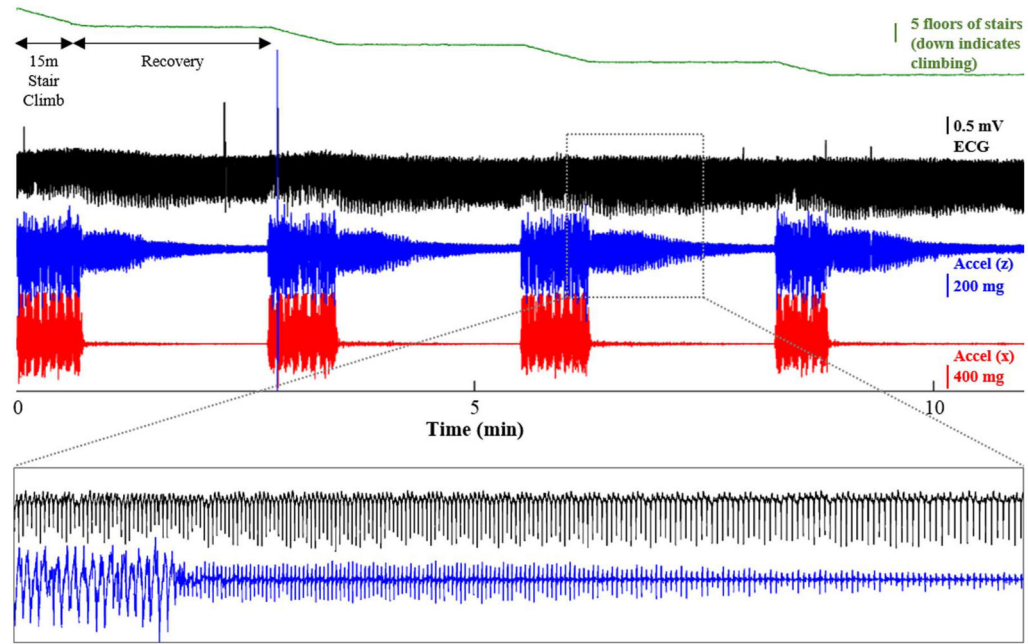


Fig. 5. All signals (from top to bottom, pressure-based height, ECG, SCG_z , SCG_x) measured from a healthy subject performing several successive stair climbing exercises. After climbing each set of stairs, the subject stands still for two minutes to recover; during that period, the SCG signal RMS power recovers to the baseline value. The height of the stairs that were climbed, z , was derived from the pressure sensor output, P , using the barometric formula: $z = -RT/Mg * \ln(P/P_0)$, where R is the universal gas constant, T is ambient temperature, M is the molar mass of Earth's air, g is the acceleration due to gravity, and P_0 is the baseline pressure (prior to the altitude change). The duration of the inset is 2 minutes.

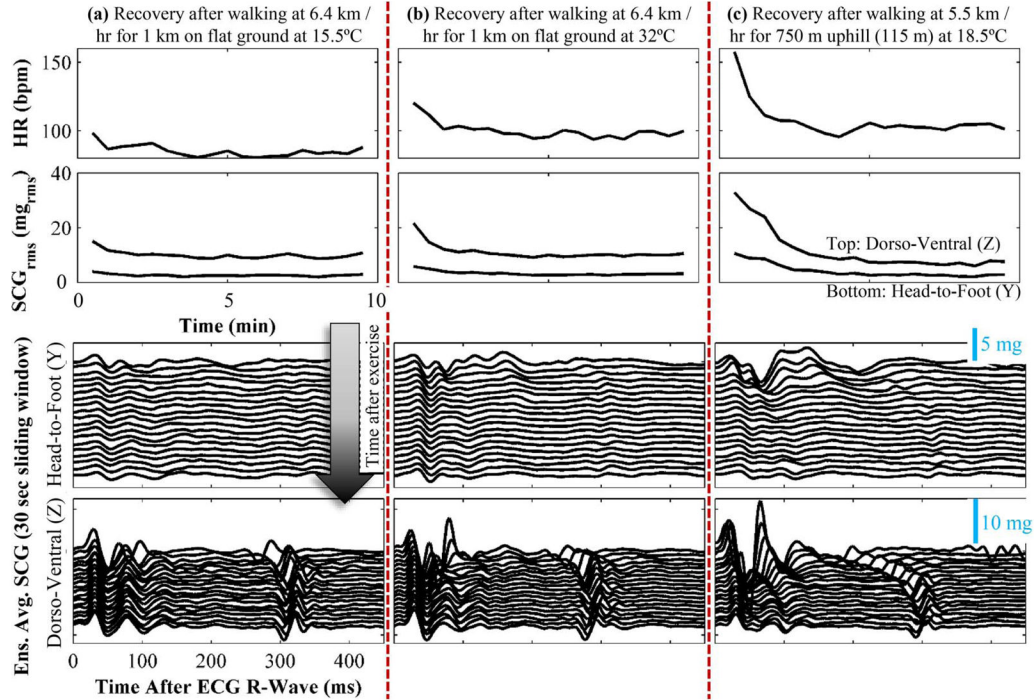


Fig. 6.

Physiological response for one subject performing three different activities described above. (a) Walking at a moderate pace in comfortable temperature with no incline produced a small increase in HR, SCG RMS power, and decrease in left ventricular ejection time (LVET) as estimated from the SCG_z (to the first order as a reduction in the time delay between the first and second complex of the SCG signal). (b) Walking at a moderate pace in warm temperature with no incline produced a much greater increase in HR, SCG RMS power, and decrease in LVET; additionally, due to the warm ambient temperature, the cardiovascular response was elevated throughout the recording (even after full recovery), demonstrated by the increased resting RMS power in the SCG_y [compared to (a)] and increased resting HR. (c) Walking at a moderate pace uphill in comfortable temperature produced the largest increase in HR, SCG RMS power, and decrease in LVET; there was also a noticeable decrease in the pre-ejection period (PEP) as seen in the SCG_z [(to the first order as a reduction in the time delay between the ECG R-wave ($t = 0$ in the plots above) to the first main complex of the SCG ensemble average)].

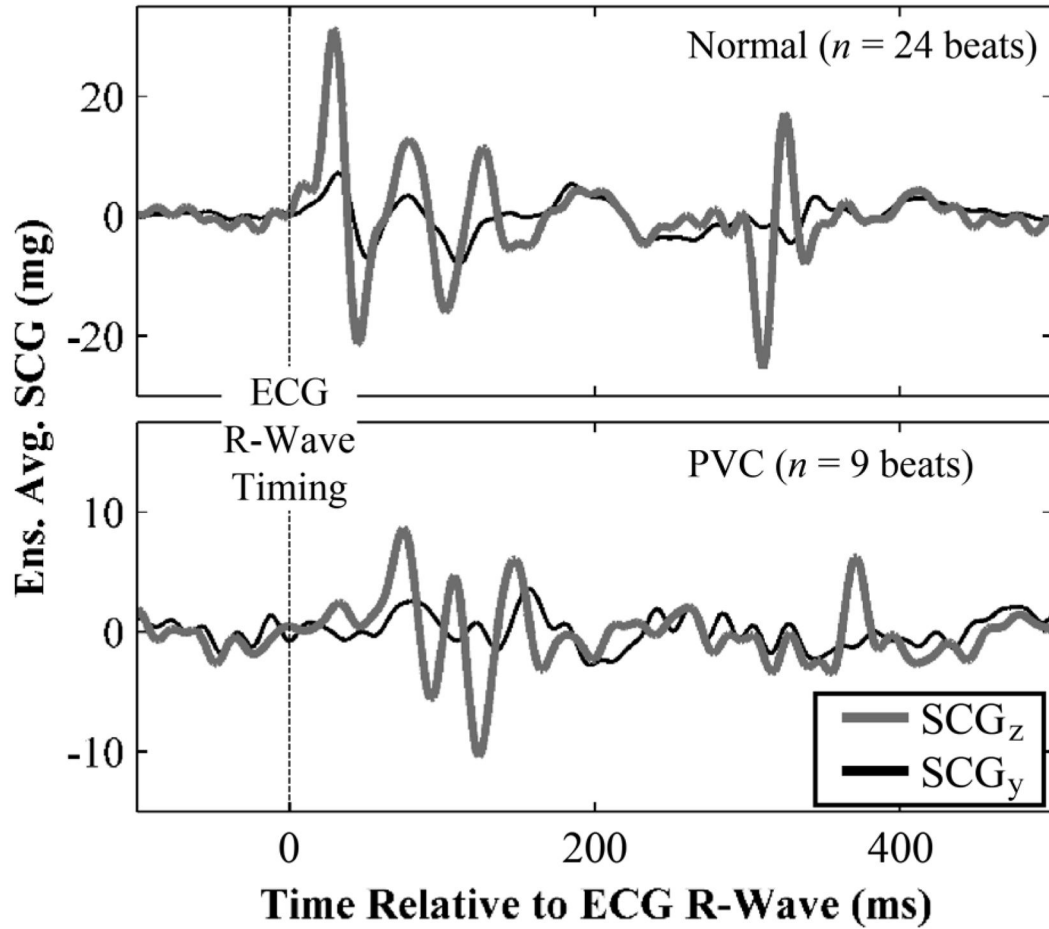


Fig. 7. Ensemble averaged SCG waveforms in the dorso-ventral (z) and head-to-foot (y) direction for normal (top) and PVC (bottom) heartbeats. Note the difference in y-axis scale for the normal and PVC beats. The time delay between the ECG R-wave and the first peak (MC) of the SCG is lengthened for the PVC beats, as is expected due to compromised contractility of the ventricle (reduced dP/dt). Interestingly, the y-direction SCG ensemble average morphology was affected more by the PVC than the z-direction, suggesting potential differences in physiological genesis for the two directions.

TABLE I

System Specifications

Parameter	Value
Overall Dimensions	9 cm × 4 cm
Physiological Measurements	ECG (single-lead), SCG (three-axis), accelerations (three-axis)
Environmental Measurements	Barometric pressure, Ambient temperature (confounded by skin temperature)
ECG Bandwidth, Noise, Sample Rate	150Hz, 8 μ V _{pp} , 500Hz
Accelerometer Bandwidth, Noise, Sample Rate	50Hz, 840 μ g _{rms} , 500Hz
Pressure Sensor Bandwidth, Noise, Sample Rate	5Hz, 0.065mbar, 10Hz
Temperature Sensor Bandwidth, Noise, Sample Rate	5Hz, 0.2°C, 10Hz
Data Storage Capacity	Limited by choice of SD card (e.g. 1 GB)
Power Consumption	7.4 mW
Battery Life (using LIR2450 battery)	50 h